Inertial Electrostatic Confinement (IEC) Device as Plasma Injection Source

Zefeng Yu

A thesis

submitted in partial fulfillment of the

requirements for the degree of

Master of Science in Materials Science and Engineering

University of Washington

2015

Committee:

Fumio S. Ohuchi
Jihui Yang

Program Authorized to Offer Degree:

Materials Science and Engineering

University of Washington

Abstract

Inertial Electrostatic Confinement (IEC) Device as Plasma Injection Source

Zefeng Yu

Chair of the Supervisory Committee:

Professor & Associate Chair, Fumio S. Ohuchi

Materials Science and Engineering

In this thesis paper, full experimental and analytical processes of cylindrical IEC plasma injection source and Langmuir probe tests are discussed. The IEC plasma injection source is constructed for DOE project to interact with SiC. Total four versions have been made, and each performance is evaluated. IEC is constructed by two cylindrical grids, which has a positive anode grid and negative cathode grid. It has been demonstrated that higher cathode grid causes higher collision rate between particles, which leads to higher plasma intensity. The radius of plasma depends on anode and cathode grid radius ratio. The higher the ratio, the narrower the plasma beam it produces. In addition, a virtual anode is observed to form within the cathode grid since the plasma beam is never actually in contact with cathode. Further performance tests of 4^{th} version illustrates lower gas pressure and extended anode grids would help plasma have less divergence. At the meanwhile, longer electron tails are formed at lower gas pressure.

Single Langmuir probe has been used to obtain IV curve to calculate electron temperature (Tev), electron thermal velocity (ve,th), and plasma density (ne). Those plasma properties have been analyzed for 4th version at 0.4'' and 0.6'' away from cathode, respectively. At same probe position, the plasma density increase as cathode voltage increases because of higher collision rate by higher potential fields between

electrodes. The result shows the optimum plasma condition is at -1.5 kV and 30 mTorr. At same cathode voltage, the plasma density increases as the probe moves to further distance respect to cathode grid. Nevertheless, the plasma density is around 10^{16} m^{-3}, which is consistent with other plasma source found in reference papers. The success of controlling plasma injecting only in one direction in a continuous plasma flow demonstrates the potential of this device to operate as a particle (electron or ion) source or small propellant thruster.

Table of Content:

1. Introduction

1.1. General Interest and Motivation:

Besides the three common states, solid, liquid, and gas, matters can exist at the fourth state that is known as the plasma. Plasma is basically a cloud of ionized particles with same numbers of ion and electron, which maintain its electrical neutrality. Over past 70 years, there have been many kinds of mechanical devices being created to generate and utilize plasma for various purposes. For examples, plasma etching, plasma sputtering for thin film synthesis and coating, and plasma light source for TV, they are all commercially available.

For advanced scientific research in outer space exploration, plasma has been focused on applications for spacecraft propulsion systems and fusion reactor. Most common plasma thrusters includes Hall Effect Thruster, Pulsed Plasma Thruster, Magnetoplasmadynamic Thruster, and VASIMR. [1-3] Compare to convectional fossil fuel thruster, plasma thruster provides huge specific impulse (Isp) and terminal velocity. In fact, NASA's deep space mission to Jupiter choose Hall thruster with Isp of 6000 – 8000 seconds, and thruster power of 180 kWe. [1-3]

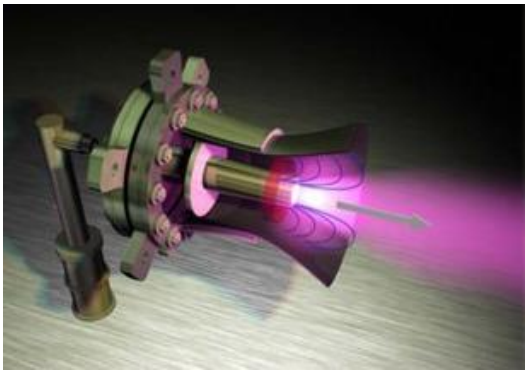

Figure 1. Magnetoplasmadynamic Thruster [3]

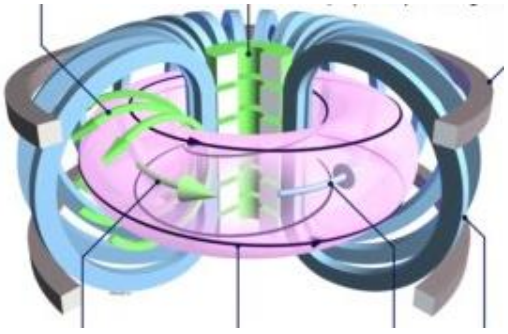

Figure 2. The Tokamak Fusion Reactor [4]

In energy source field, plasma also played in a main role for fusion reactor. For example, the Tokamak reactor, shown in Fig. 2, utilizes high temperature and energetic plasma to facilitate fusion reactions. In addition, there are many other types of fusion reactors involves plasma, and Inertial Electrostatic Confinement (IEC) Fusion reactor was one of them. The Department of Energy also interested in a device named Magnetohydrodynamics (MHD) to generate electricity from a continuous flow of plasma. Either the plasma for spacecraft thruster or energy source, there will be potentially material corrosion done by hot plasma. Therefore, the concern of material interaction with plasma initiates this master research project to characterize material impact done by high energy plasma.

Professor Ohuchi used to corporate with people at Redmond plasma lab under AFORS and NASA sponsor. Previous master student, DuWayne Smith, has constructed a FRC plasma source over there. However, due to sponsor termination, the FRC project was shut down and the device was dissembled. Therefore, I need a new plasma source for my interest in plasma science. At the meanwhile, a new DOE project was assigned to a Phd student in our group to characterize SiC interaction with plasma for MHD purpose. Therefore, my master research in developing a new plasma source will be corporate in the new DOE project. Hence, my overall project goal was to design and construct my own plasma source, which I chose to be IEC plasma, and analyses plasma properties. If it has high enough density and focus, we will use my plasma source in the OG chamber to radiate SiC, and characterize it. However, due to the complexity of plasma science, my research will focus on plasma source construction and property analysis.

1.2. Background of Plasma Science:

To understand every aspects of plasma science, ones need to obtain a great comprehension of radiation transport, excitation, ionization process, and chemical reactions. [5] Despite, the abstruse of plasma science, it is straightforward to understand some fundamental plasma principles and mechanisms. As stated in the beginning of this paper, matter in the state of plasma is not an easy and common process. It usually requires high energy to ionize gas or fluid atoms to initiate plasma discharge. Usually, there are two categories of plasma initiation sources, Radio Frequency (RF) plasma and Direct Current (DC) plasma. RF plasma sources utilizes radio frequency to oscillate atoms around magnetic field to cause ionization. Our attention will focus on DC plasma source, because IEC plasma is one DC plasma branch.

The most straightforward way to generate plasma is to ionize background neutral gas atoms by applying high voltages between two electrodes, as shown in Fig. 3. When the voltage potential difference exists between cathode and anode, following electrical

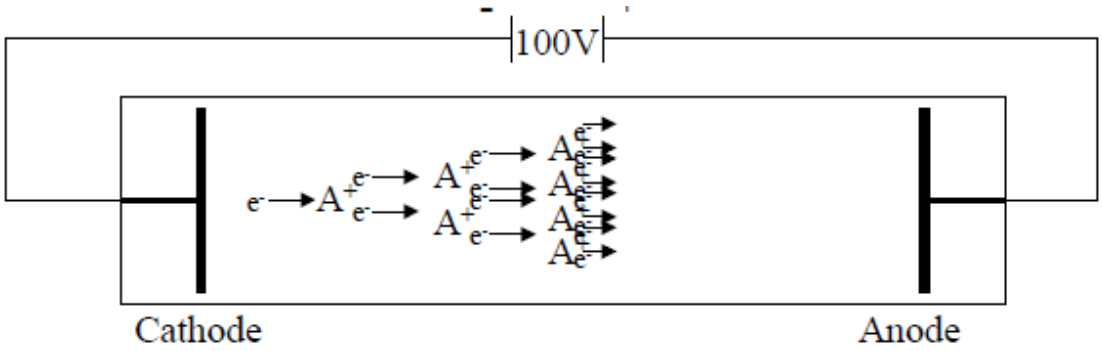

Figure 3. Mechanism of DC glow discharge diagram [6]

field, some free electrons emitted from cathode will be on way to anode and collide with background neutral gas to causes ionization which emits additional secondary

electrons. Now more electrons are on the way to anode and collide with more neutral atoms. This electron avalanche causes and maintains plasma glow discharge.

To generate DC plasma, it usually follows Paschen curve, as shown in Fig. 4, which has pressure times electrode spacing as the x-axis and breakdown voltage as the y-axis. Plasma can only form at certain pressure, electrode spacing and corresponding voltage. The background neutral gas atoms usually use inert gases, which follow their own Paschen curve. It is important to generate your own Paschen curve for your device because it may vary depends on various devices and experimental conditions.

1.2.1. Mechanisms of Magnetohydrodynamic (MHD)

Since my research will be incorporated in the DOE project for MHD interaction materials, it is important to understand some fundamental MHD principles and mechanisms. The conventional way to generate electrical power is from hot vapor driving large turbines. The process involves huge thermal and mechanical energy loss. MHD, on the other hand, uses moving plasma that going through magnetic field to extract out electrons through electrodes. The high kinetic energy of flowing plasma is directly converted to electric energy, which dramatically enlarges the efficiency. [8] When the gas is going through magnetic field and causes magnetic flux changes, according to Faraday's law of induction, it results in electromotive force on electrons as shown in Fig 5. Then, the electron is extracted out through electrode material, in our case is the SiC. For mathematically principles, the ideal MHD must satisfy Maxwell equations, mass conservation, adiabatic equations for fluids, and ideal Ohm's Law for

fluids. [8] The equations are shown in Fig. 6. However, we are not interested in detail mathematical calculations.

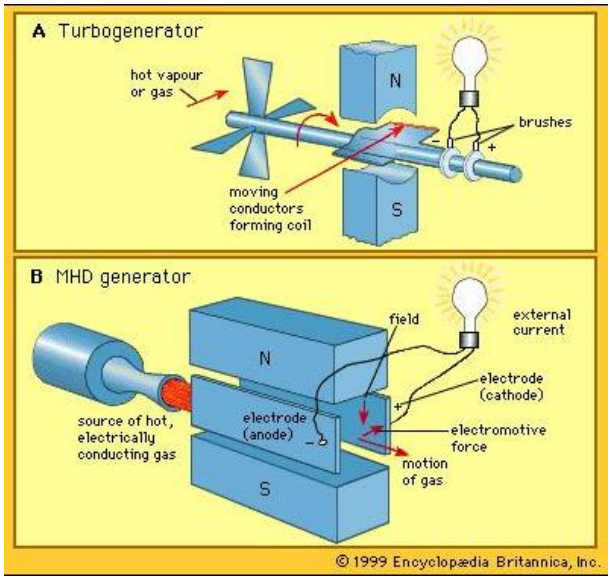

Figure 5. Turbogenerator vs MHD [8]

Ideal MHD Condition:

$$\frac{\partial \mathbf{B}}{\partial t} = -\nabla \wedge \mathbf{E}$$

$$\frac{\partial \rho}{\partial t} + \nabla.(\rho \mathbf{v}) = 0$$

$$\rho \frac{d\mathbf{v}}{dt} = -\nabla p + \mathbf{j} \times \mathbf{B}$$

$$\nabla \wedge \mathbf{B} = \mu_0 \mathbf{j}$$

$$\frac{d}{dt}\left(\frac{p}{\rho^{\gamma}}\right) = 0$$

$$\mathbf{E} + \mathbf{v} \wedge \mathbf{B} = 0$$

Figure 6. Ideal MHD equations.[8]

1.2.2. Mechanism of Inertial Electrostatic Confinement (IEC) Plasma

From the experience of my senior project with DC plasma, I have learned that it is difficult to control the shape and focus point of plasma beam by only using two capacitor plates. Since our project goal is to interact material with plasma, it is necessary to be able to control plasma shape, direction, and parameters easily. Therefore, I came up with using IEC plasma as our new plasma source, due to its controllable parameters and simplicity for construction and testing.

Robert L. Hirsch had constructed an IEC plasma generator in 1970s with ions acceleration inwards. As shown in Fig. 7 a), a spherical anode with large radius is placed outside, and grounded. Another spherical cathode with smaller radius set inside the anode with high negative voltage. [10] The cathode is assumed to be transparent to both

ions and electrons because the distance between wires are larger than electron Debye length. The Electrical field points inwards so that ions travel inwards along the E field. Then, they will eventually arrive at center of the grid to form plasma. The detailed processes of plasma formation inside the cathode is as described as following, and shown in Fig. 8, [10-11]

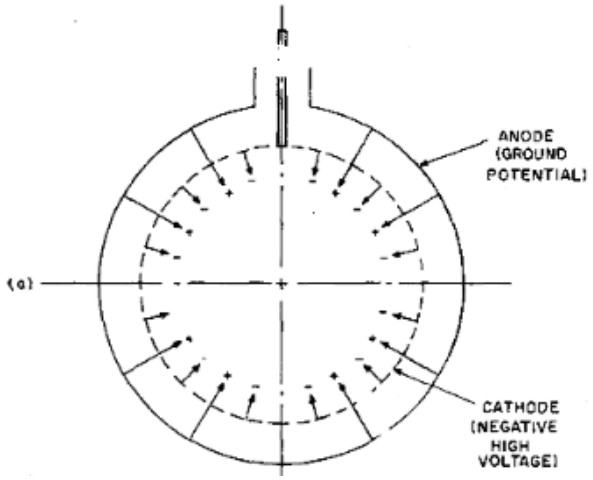

Figure 7. a) IEC by Robert L. Hirsch diagram [10]

① Electron impact of ionization first starts at region between electrodes.

② Formed ions then follows E field and accelerated inward.

③ Because of high mesh transparency of inner grid, energetic ions will pass through cathode grid.

④ Then those ions will further bombard with more neutral particles and ionize them, and then causes secondary electron emission.

⑤ At meanwhile, ions decelerate and form virtual anode inside cathode.

⑥ Secondary emitted electrons will be trapped inside cathode to maintain discharge.

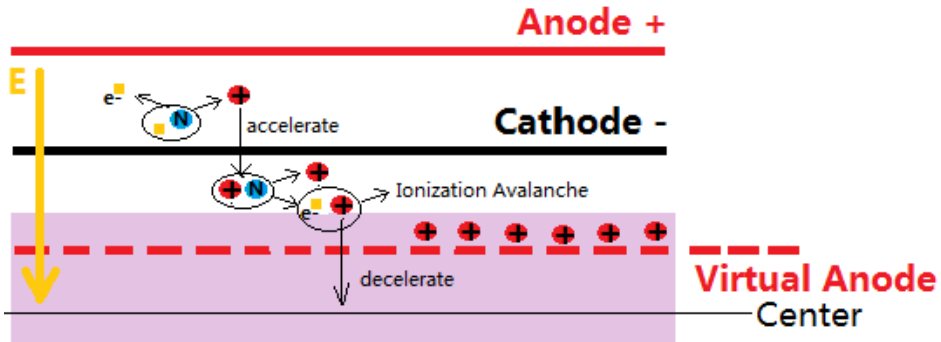

Figure 8. Plasma confinement processes within grids

Overall, IEC with spherical grids have two modes, Star Mode and Jet Mode, as shown in Fig. 9. The Star mode is formed under certain gas pressure, grid voltage, grid configurations, and most importantly grid symmetry. The inwardly accelerated ions, described in above paragraph, will create space-charge-neutralized ion beams, named "Microchannels". [15] Those microchannels guide ions to converge in the center of the grid with minimum ion corrosion and collision with the grid. Under high grid symmetry with uniform potential field between the grids, the plasma will focus and remain at the center within cathode.

If the local potential field is distorted between grid by nonsymmetrical design, Jet mode start to kick in. Ions are injected outward because of local gradient causes electron flow outwardly, which initiates intense space charge neutralized ion beams at

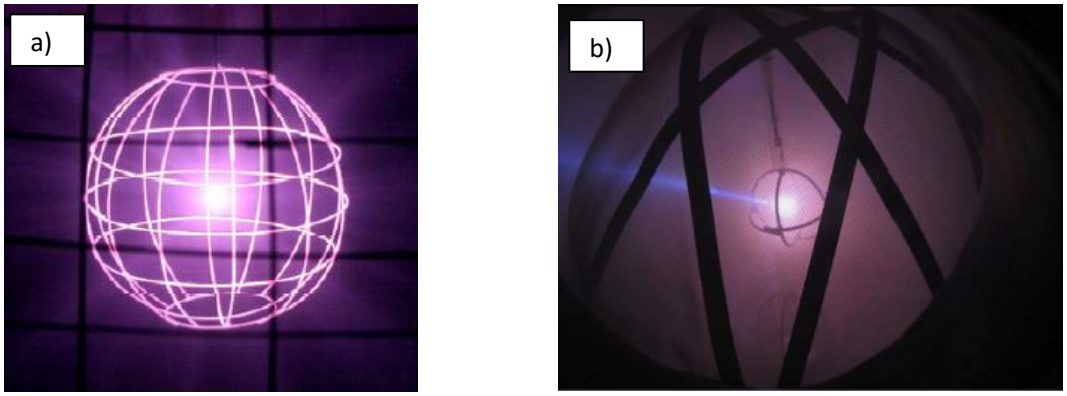

Figure 9. a) IEC Star Mode b) IEC Jet Mode [13 – 14]

that location. [15] It has been demonstrated that half of the energy pass on to ions in the microchannels is directly transferred into plasma injection beam. [15]

Recall our project goal is to direct plasma to interact with interested material. Therefore, the jet mode of IEC plasma is chosen to match project purpose. In addition, I have chosen a double cylindrical grids configuration instead of double spherical grids to

generate plasma beams. Even though the non-symmetry can extract plasma outward from spherical cathode, it is mechanically difficult to build perfect spherical grids with large open hole, and difficult to make sure that the plasma will only leak through that large open hole, not in multiple directions. It would be much easier to use cylindrical configuration to both confine the plasma and direct it outward, which has been tested by UW-Madison for fusion confinement purpose.

1.2.3. Single Langmuir Probe Diagnostics

Langmuir probe was named after the Nobel Laureate Irving Langmuir for his invention of using a metal probe to measure current-voltage (IV) curve in order to extract out useful plasma properties. [16] Nowadays, Langmuir probe becomes a fundamental tool to measure electron temperature (Tev), thermal electron velocity (ve,th), and plasma density (ne). Also, it has evolved from single probe to double probe and emissive probes. [16-18] However, for my incipient study of IEC plasma source, I will only use single Langmuir probe for the experimental simplicity.

Even though the mathematics and theory behind Langmuir probe is complicated, the setup of it is relatively easy. It is basically a shielded metal bar with only the tip exposing to plasma. At the meantime, the probe is biased to a DC power supply sweeping from negative to positive voltage, and in series with an ampere meter to measure current at each sweeping voltage. An ideal IV curve is shown in Fig. 10. [16] A simplified circuit diagram for probe measurements is also shown in Fig. 11. [19] It is important that most of the probe body is insulated from plasma to avoid any

measurement interference. The common probe material is Tungsten wire because of its high corrosion resistance, thermal stability, and good conductivity.

In order to get useful information from IV curve, one needs to understand how the probe works under plasma influences and what each segments of IV curves represent. The mechanism of probe is based plasma sheath theory. Plasma sheath a region that is electrons depletion and ion rich around probe. It is plasma sheath that allow either attract or repel electrons and ions to collect plasma properties. [16-20] Details

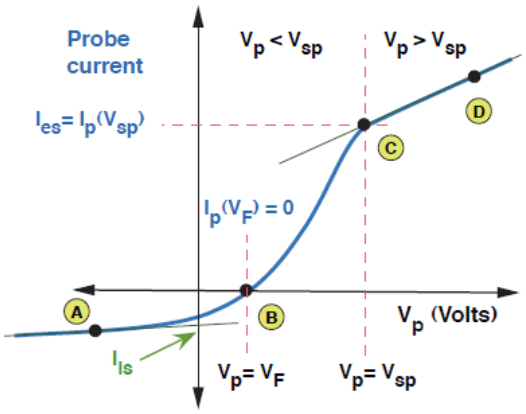

Figure 10. Ideal IV Curve [16]

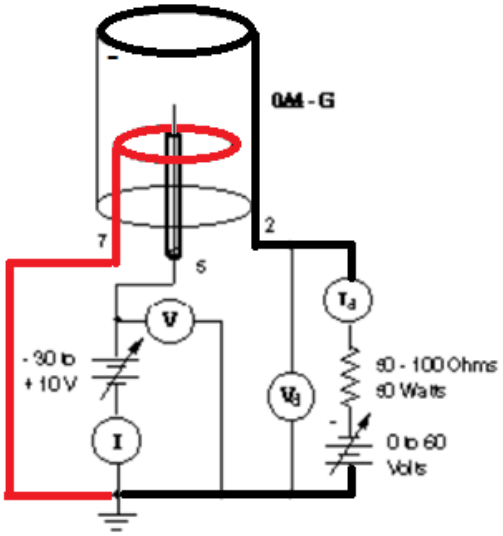

Figure 11. Langmuir probe setup [19]

will be explained when we take closer look at each IV curve sections.

As shown in Fig. 10, the IV curve has three main sections. Vp is the probe voltage that sweep from negative to positive. Ip is the probe current, which Ip = Ie + Ii. V_F is floating voltage that ion current (Ii) equals electron current (Ie) to cancel out each other. Vsp is plasma potential, and its corresponding current is electron saturation current, Ies.

First section is A-B, starting from very negative potential to V_F. When the probe is extremely negative, because electron has negative charge, probe repels away all

electrons, but attract ions. The schematics is shown in Fig. 12. [16-18] The probe current is dominated by ion current, Ii, [18]

$$I_i = -I_{is} = \frac{1}{4} e n_i v_{i,th} A_{probe} \qquad (1)$$

where, A_{probe} is probe area, and $v_{i,th}$ is ion thermal velocity, [18]

$$v_{i,th} = v_{Bohm} = \sqrt{\frac{kT_e}{m_i}} \qquad (2)$$

As the probe potential approaches V_F, ion pre-sheath starts to form. Some of energetic electrons at bulk plasma region will across sheath boundary and being detected by the probe. That is why the current start to be less negative.

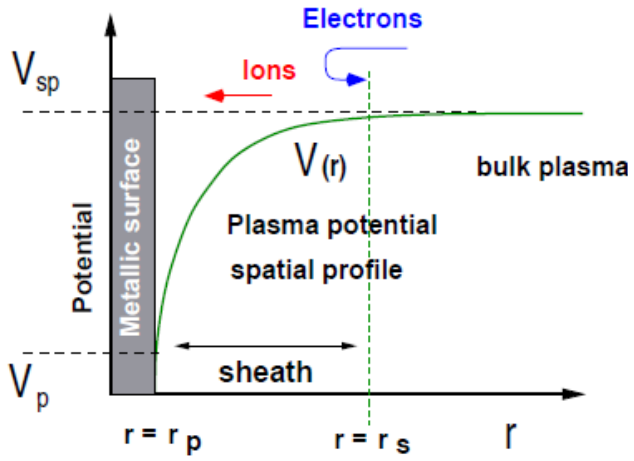

Figure. 12. Negative probe potential [16]

Second sections is B-C, where $V_F < Vp < Vsp$, plasma sheath will start to form and shrinks as the probe voltage increases. Since the probe voltage is still smaller than plasma potential, the schematics is still same as shown in Fig. 12, but with smaller sheath thickness as more energetic electrons across the boundary to causes exponentially increases of IV curve. The corresponding mathematical expression of electron current, Ie, [16-20]

$$I_e(V_p) = I_{es} exp\left(-e\frac{V_s - V_p}{kT_e}\right) \qquad (3)$$

At the point of Vp = V_{sp}, there is no potential difference and no electric field, which means no space charge shield. The migration of particles to probe is due to their thermal velocity. Therefore, we can related electron thermal velocity, $v_{e,th}$ to T_{eV},

$$v_{e,th} = \sqrt{\frac{8kT_e}{\pi m_e}} \qquad (4)$$

In addition, floating potential, V_F, can be expressed in term of Tev, [18]

$$V_F = V_p + T_{ev} ln\left(0.6\sqrt{\frac{2\pi m_e}{m_i}}\right) \qquad (5)$$

At plasma potential, the corresponding current is electron saturation current, Ies, and can be mathematically expressed as, [16-20]

$$I_{es} = \frac{1}{4} e n_e \vec{v} A \qquad (6)$$

For section, C-D, staring from point C, the probe voltage starts to excess plasma potential. Therefore, relative to plasma, the probe is at positive and attracts electrons as shown in Fig. 13. [16] Therefore, electron sheath will form around probe and expands as probe voltage increases to attract more electrons. The IV curve shows an exponentially decreasing trend for this section which similar to the spatial fluctuations of the plasma potential around a point charge,

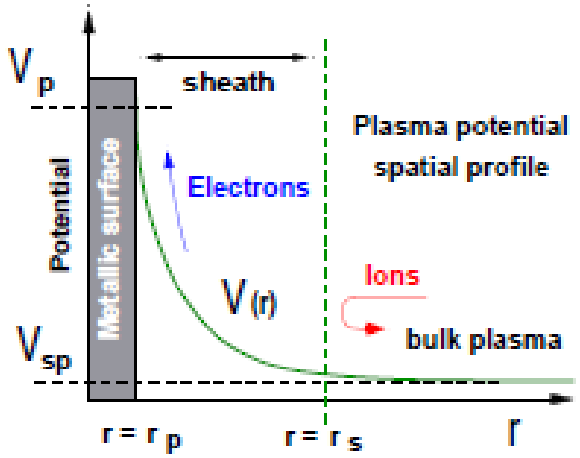

Figure. 13. Positive probe potential [16]

$$\delta V_{sp} \sim (1/r) \times exp(-r/\lambda_D) \qquad (7)$$

2. Experiments:

2.1. Plasma Chamber Setup

The Plasma Chamber consists a main cylindrical chamber (10'' in diameter, 28'' in length), three pressure gauges (TC gauge, Baraton gauge, Cold cathode gauge), two high power supplies, two rough pump (EDWARDS IEC 34-1, GENERAL ELECTRIC MOD 5KC36PN435AX), one turbomolecular pump (Alcatel MDP 5011), and a variables value. The chamber full view and construction diagram are shown in Fig. 14 and Fig. 15, respectively.

Main Vacuum Chamber :

- Pressure gauages
  - Cold cathode (A)
  - TC gauge (B)
  - Baratron gauge (C)
- 2 high power supply. (D)
- Gas value (E)
- Confinement grids (F)
- Extracting probe (G)
- Rough pump (H)
- Turbo pump (I)

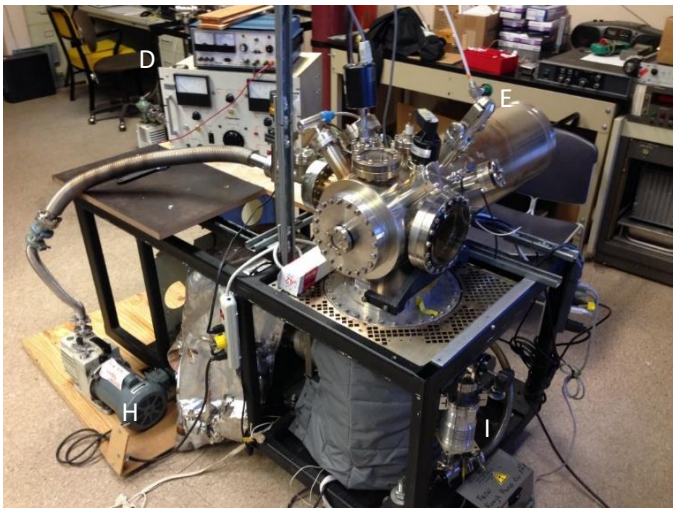

Figure. 14. Full Chamber View

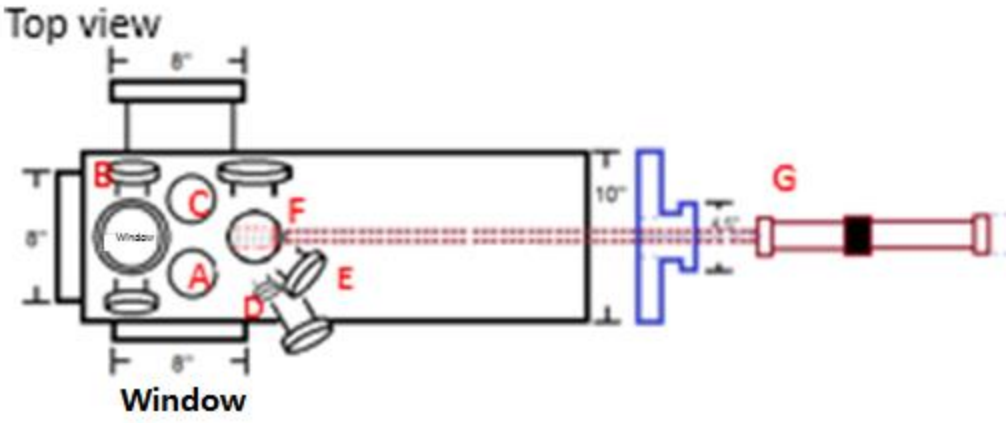

Figure 15. Top View of Plasma Main Chamber

2.2. Plasma Grid Designs

IEC plasma utilize potential fields to ionize gas particles, therefore, it is important to have strong and uniform potential fields between electrodes. In my design, two cylindrical grids with an outer positive grid and inner negative grid have been constructed for the purpose of plasma injection. Totally four version of cylindrical IEC device had been made, and shown in Fig. 16. The 4th version is the finalized device for plasma density tests and potential device to be used for our DOE project.

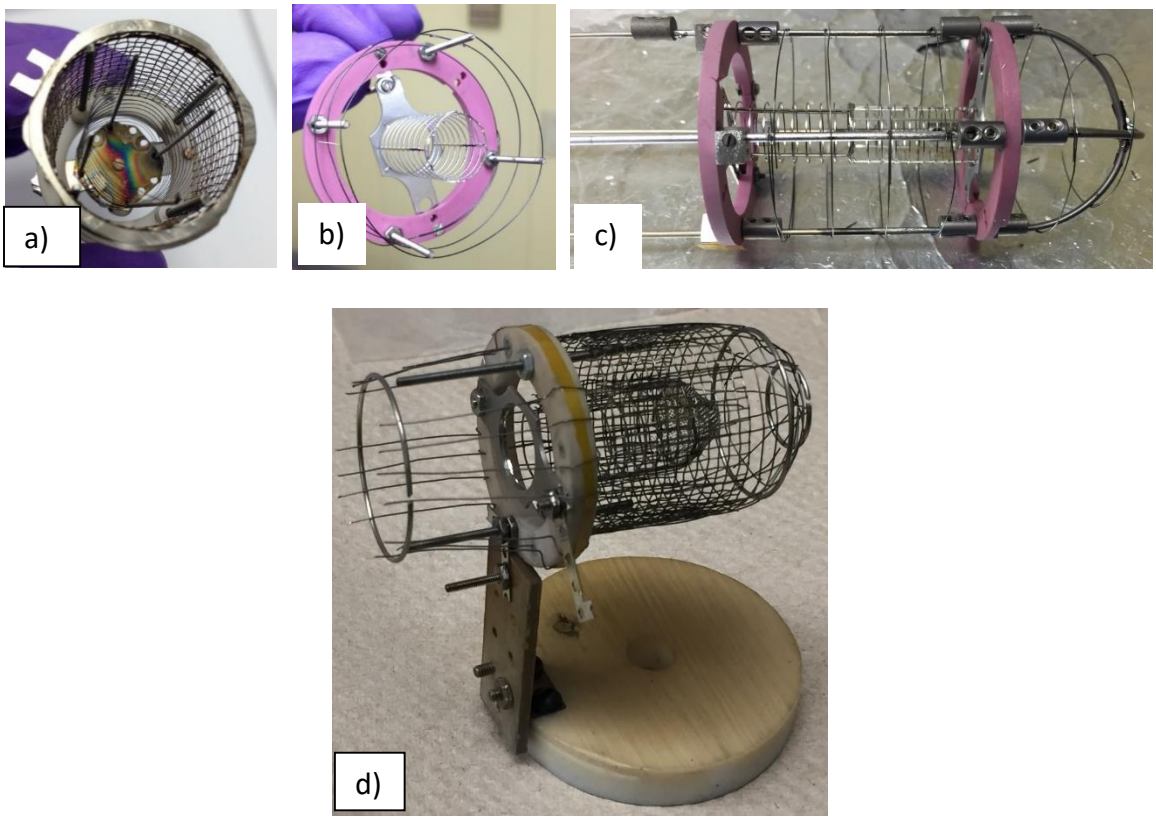

Figure 16. Cylindrical IEC Plasma Injection Device. a) 1st version (r+/r- = 2:1) b) 2nd version (r+/r- = 4:1) c) 3rd version (r+/r- = 4:1) d) 4th version (r+/r- = 2:1)

The outer grid to inner grid ratio varies through 1st to 4th version. The changes in grid radius ratio is expected to change plasma density and electron temperature since potential field have been altered and ions would have different velocity to enter into

cathode grid. Therefore, the ratio of grids' radius and the radius of cathode itself would all affect plasma properties.

As Fig. 16 shows that the design of 1st version has evolved from two cylindrical grids set concentrically to 4th version that has one end closed by half spherical grids. The reason is that plasma will inject outward in both direction if it is not capped on. Therefore, 1st and 2nd version would have plasma injection in both direction, which we do not want it to happen. Although 1st and 2nd version is not desirable, it would still be the first important step to check whether the cylindrical confinement of plasma works or not. 3rd version has a half spherical gird on anode end, unfortunately, the plasma still shoot out. Only the 4th version with both cathode and anode capped on, the plasma is injected in one direction. Detailed performance of those devices will be shown and discussed in later sections.

2.3. Langmuir Probe Test Setups

Langmuir probe is driven by its own grounded DC power supply. The sweeping voltage is measured with respect to ground. When the voltage is either below or above plasma potential, the currents will behavior as we have discussed above.

There are two testing setups have been done. In Fig. 17 a), the position of probe is fixed at 0.4'' away from cathode, and IV curves are measured with cathode voltage at -1000, -1250 and -1500 volts, respectively. The corresponding data analysis would indicate plasma properties changes as cathode voltage increases. In Fig. 17 b), the cathode voltage is fixed, and the IV curves are measured with probe position at 0.4'' and

0.6'' away from cathode. Therefore, the plasma properties would be checked as the beam is injecting out from the confinement. Anode is fixed at 200 volt and background pressure is chosen to set at 30 mTorr because of plasma divergent effect.

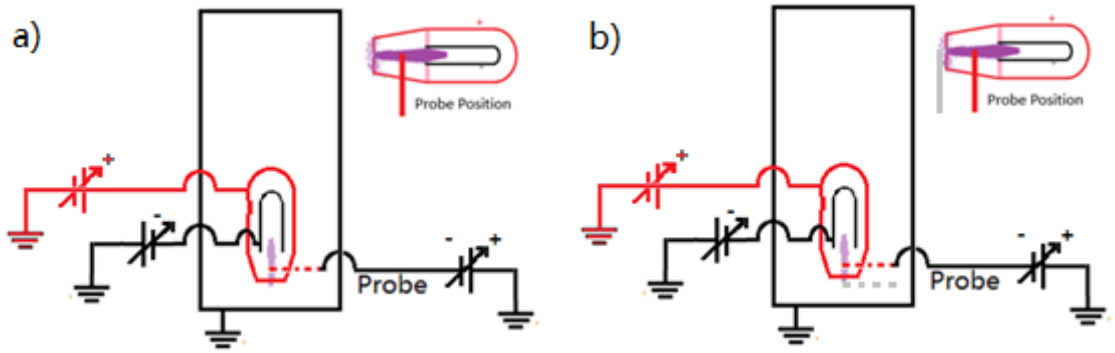

Figure. 17 Langmuir probe a) position fixed b) position varies

3. Results and Discussion:

3.1. Visual Performances of Plasma Beam

Based on all the IEC theories and reference materials discussed above, the first step is to test out whether cylindrical grid would confine plasma in the center, which has been illustrated in Fig. 18 for 1st and 2nd version as voltage increases respectively.

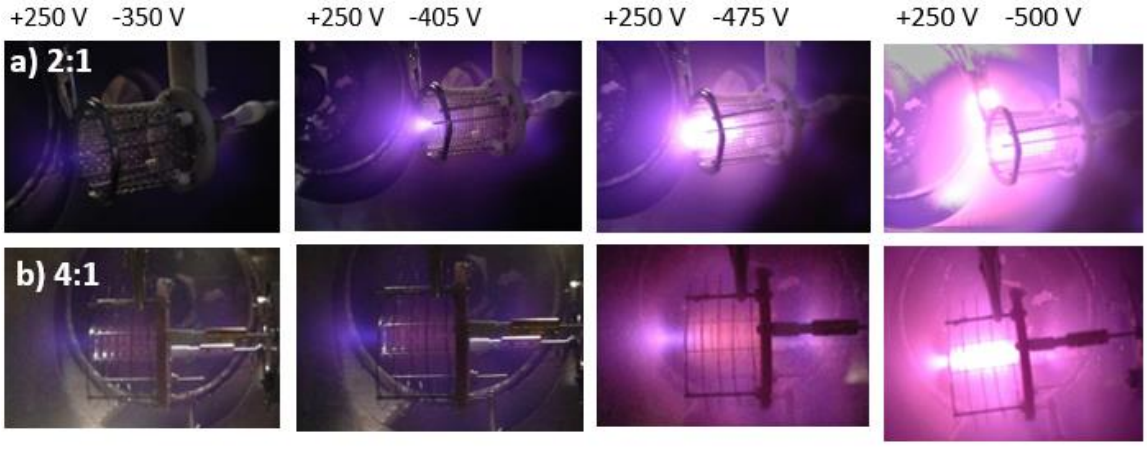

Figure 18. Plasma confinement of a) 1st version vs b) 2nd version as voltage increases

As the voltage increases, the potential fields between electrodes should increase as well. Higher potential fields would lead to higher ion acceleration, which causes more ions and background gas particle to collide. Hence, the increased collision rate eventually causes electron avalanche and increased plasma density. Therefore, brighter and larger diameter plasma beam was observed for both versions.

The enlarged plasma radius of 1st version with radius ratio of 2:1 is illustrated in Fig. 19. Since the final 4th version also have radius ratio of 2:1, it is necessary to examine the plasma radius change. The increased radius is not perfectly linear, as shown in Graph 1. The linear fit equation gives us, $y = 0.0017x - 0.9141$, for radius and plasma breakdown voltage relationship.

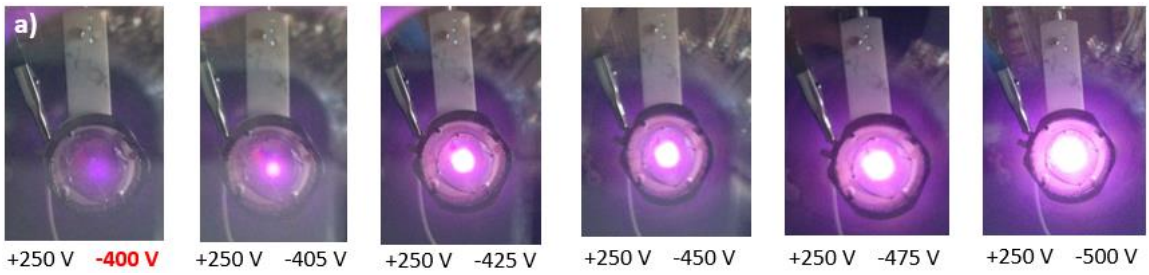

Figure 19. Plasma Radius of 1st version as voltage increase at 130 mTorr

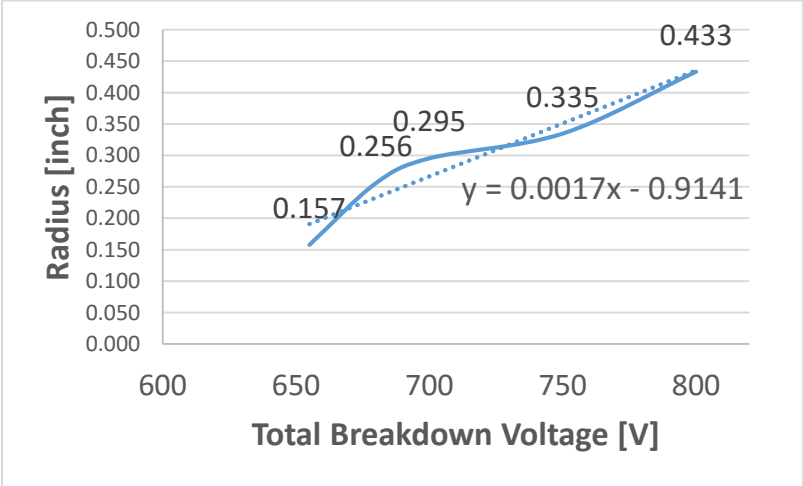

Graph 1. Plasma Radius vs Total Breakdown Voltage of 1st version with radius ratio 2:1

Above described experiment operated at pressure of 130 mTorr, which is much higher than 3rd and 4th version's tests for Langmuir probe tests. Since, the pressure is much high, according to Paschen Curve, the corresponding plasma breakdown voltage would be low at millitorr range. Therefore, much lower voltage could be used to initiate plasma beams. However, the divergence of plasma once it leaves confinement grids was significant. Lower pressure and extended grid in 3rd and 4th version would help plasma beam to focus more.

3.2. Visual Performance of 3rd and 4th Version

To prevent plasma injection in both ends and plasma divergence, half spherical grid is added to 3rd and 4th version. As Fig. 20 shows plasma injection in one direction for 3rd version, the extended grid of anode indeed assist to cancel out divergence as voltage increases. The Plasma beam also becomes more intense at higher voltage because of higher collision rate. However, there were still several issues about 3rd version design, for example a metal sheet that fix cathode concentrically to anode causes the heart shape plasma at 600 V breakdown voltage in the last picture in Fig. 20.

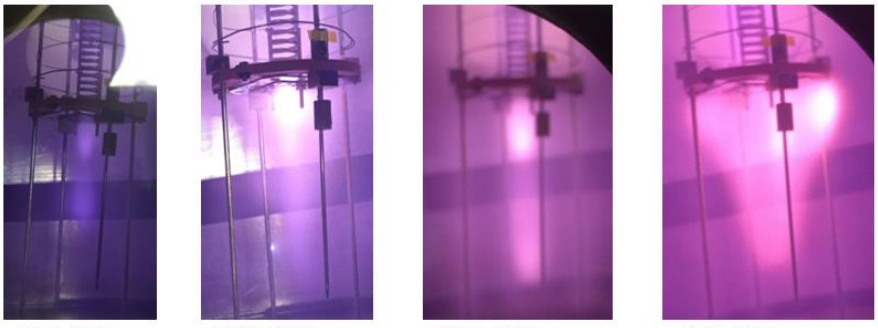

Figure 20. Plasma confinement of 3rd version as voltage increases at pressure 44mTorr

In addition to metal sheet problem that can be fixed to use high ceramic material, the plasma beam actually shoot in the opposite direction as well, despite the added half spherical grid on anode in Fig. 21.

Figure 21. Plasma injection despite of spherical grid on anode at pressure of 44mTorr

To correct those problems, 4th version has been constructed as the final version so far. To make sure that all plasma is propelled only in one direction, another half spherical grid is added to the cathode. Hence, with two half spherical girds on one end, it should behave as spherical IEC designs with large opening holes. Once the plasma is formed inside cathode half spherical grid, the plasma tends to find large week potential fields to escape from confinement. Therefore, as shown in Fig. 22 and Fig 23, plasma shoot out in only one direction in each tests.

Figure 22. Plasma injection of 4th version as pressure varies from 80 to 30 mTorr

Those test is conducted at fixed cathode and anode voltage while pressure drops from 80 to 30 mTorr. Obviously, the divergence of plasma drops dramatically at lower

pressure because there are less collisions between ions and electrons which causes focusing of ions in one direction. [14] Less electrons with lower energy will be repelled by interparticle electrostatic repulsion force to causes beam split symmetrically. Therefore, the divergence will more likely to disappear if lower pressure is applied. [14]

Beside less divergence of plasma is confirmed at lower pressure, a longer beam tail is observed as pressure decreases. This tail is primarily consists of lower energy electrons. When pressure drops, less collisions happen in the confined core because therefore are less background gas atoms. However, some electrons still have enough energy to overcome negative cathode field and escape from grid. [14] Therefore, a longer electron tail was formed at lower pressure.

At fixed pressure of 30 mTorr, the plasma is observed to increase intensity as cathode voltage increases, which is consistent with previous experiments. At the highest cathode voltage of -1.5kV, 4th version reaches its highest plasma intensity, and the plasma tail is the longest as well. Since the project goal is to extract plasma out from confined grid and to focus plasma beam onto material for radiation, 4th version operating at 30 mTorr and cathode voltage of -1.5 kV is best condition to achieve maximum plasma radiation.

Figure 23. Plasma injection of 4th version as cathode voltage increases

3.3. IV Curve Analysis of 4th Version

3.3.1. IV Curve Analysis Procedure

Step 1, Get typical IV curve:

The very first thing is to get an accurate IV Curve with a deflection point on the positive probe voltage side. As probe current increases exponentially, at the deflection point, the slope of the line should decreases. This deflection point is important because it tells us where the plasma potential, Vsp, and electron saturation current, Ies are at.

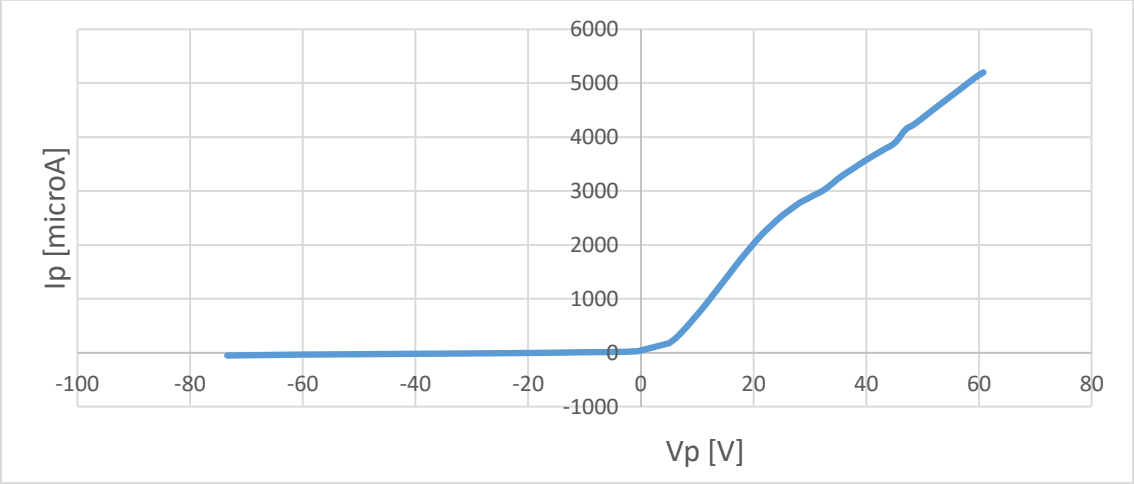

Graph 2. Typical IV Curve with deflection point at -1000 Cathode Voltage

Step 2, Tendency for ion saturation current, Iis:

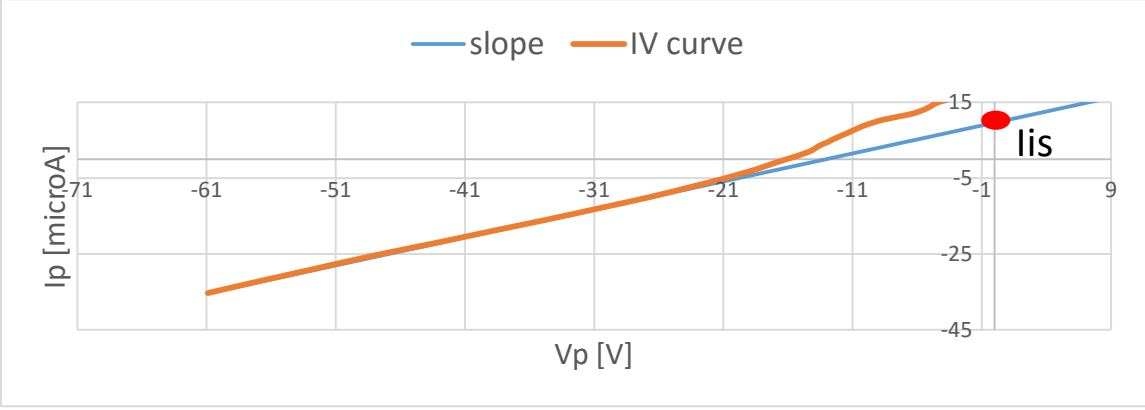

Graph 3. Tangent line for ion saturation current, Iis

Step 3, Get probe floating voltage, V_F :

Floating Voltage is where the ion current equals to electron current. Therefore, the probe voltage should be 0, and can be easily get from IV Curve. It is important to get an accurate V_F because we then can use eq. 5 to calculate Tev. [18]

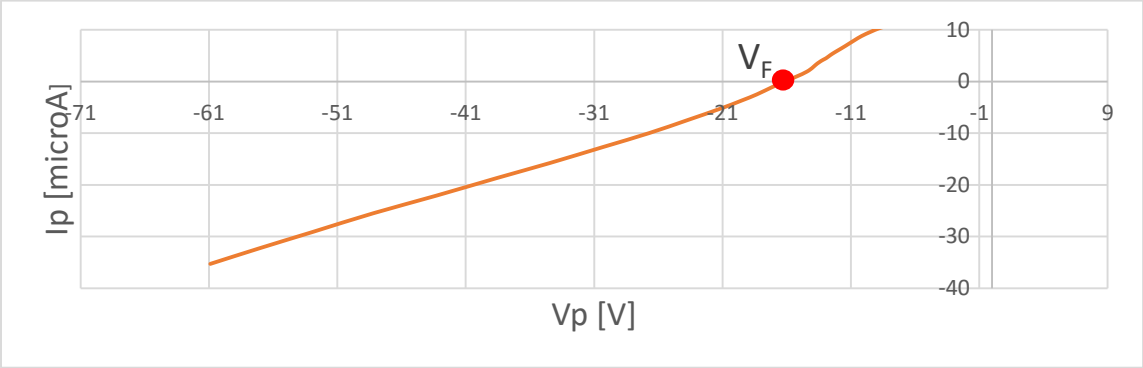

Graph 4. Getting floating voltage at where probe current equals zero.

Step 4, Subtract Iis from Ip to get Ie(Vp):

Since we are calculating plasma density in term of electron, it is necessary to eliminate any ion effects on current. Therefore, Iis should be subtracted from total probe current to obtain electron current as probe voltage varies.

Step 5, Get Tev, Ies, and Vsp from slope of Ln(Ie)

Another common method to get Tev is from calculating the slope of ln(Ie) based on eq. 3, which becomes,

$$ln\left(\frac{I_e}{I_{es}}\right) = \frac{e}{kT_e}\left(V_p - V_s\right) \quad , \quad \text{where } \frac{1}{T_{ev}} = \frac{e}{kT_e} \qquad (8)$$

Therefore, the Tev is inversely proportional to the slope of the range that electron becomes saturated. Graph 5 shows a clear illustration to get Tev from slope 2.

In addition, as Graph 5 shows, the interaction of slope 1 and slope 2 gives Ies and Vsp. Then, Tev, Ies and Vsp are substituted into eq. 4 and 6 to calculate $v_{e,th}$ and n_e .

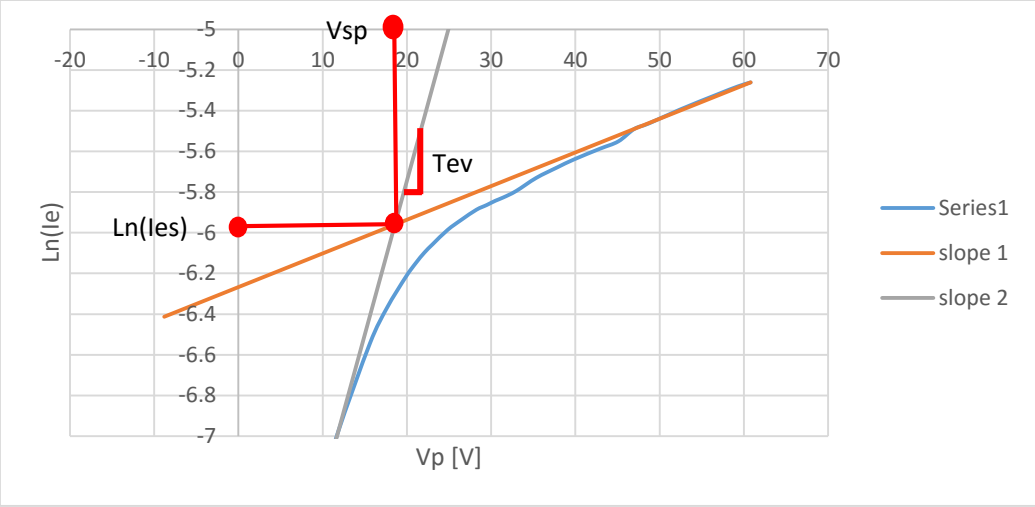

Graph 5. Get Tev, Ies, Vsp from Ln(Ie) vs Vp

3.3.2. IV Curve as Cathode Voltage Varies at 0.4''

First Langmuir probe test of 4th version measures plasma properties changes as cathode voltage varies at -1000, -1250, and -1500 V at same position, 0.4'' away from cathode. The raw data sets of IV curve is shown in Graph 6. As the cathode voltage becomes more negative, higher potential field enables more productions of electrons, which has being detected by the probe and shown as steeper slope.

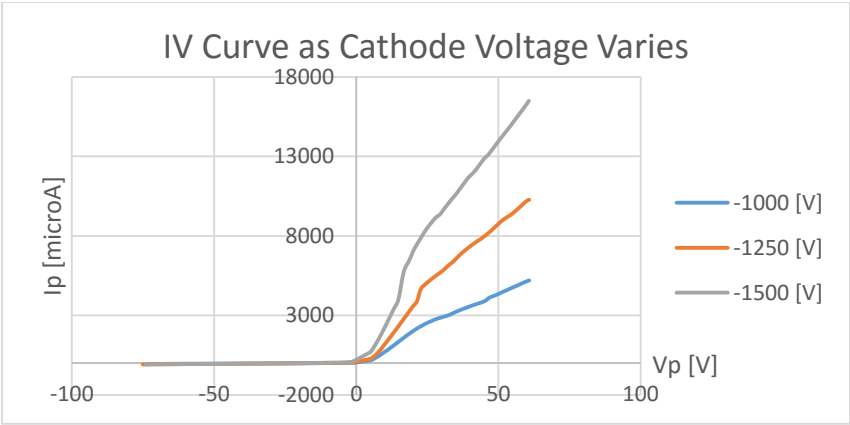

Graph 6. IV Curve of 4th version as cathode voltage increases

Take a closer look at the negative probe region in Graph 7, there is a tendency of higher cathode voltage, more negative the current it is. Recall that the current is

predominated by ions. Therefore, higher potential fields will also produce more ions, which causes the IV curve becomes more negative.

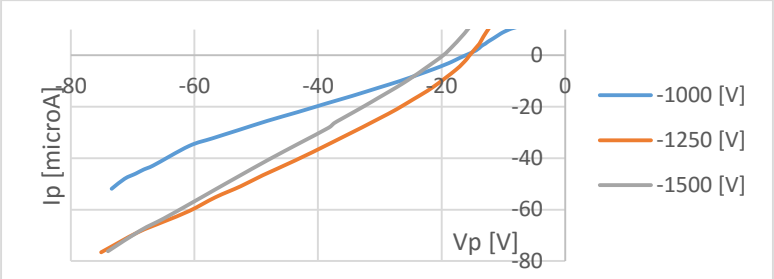

Graph 7. Negative probe region to examine Iis changes as cathode varies

It is expected that higher cathode voltage should increases the particle collisions within cathode grid, the plasms density should increase as well. A total summary of plasma properties as cathode voltage varies are shown in Table 1 and Graph 8 for the two methods described above.

	Slope Method			Vf Method		
Vc [V]	1000	1250	1500	1000	1250	1500
Te [eV]	8.04	7.74	5.28	7.07	7.10	6.10
ve,th [m/s]	1.90E+06	1.86E+06	1.54E+06	1.78E+06	1.78E+06	1.65E+06
ne [m^-3]	5.92E+15	1.23E+16	2.16E+16	6.31E+15	1.29E+16	2.01E+16

Table 1. Plasma properties summary of 4th version at 0.4'' away from cathode

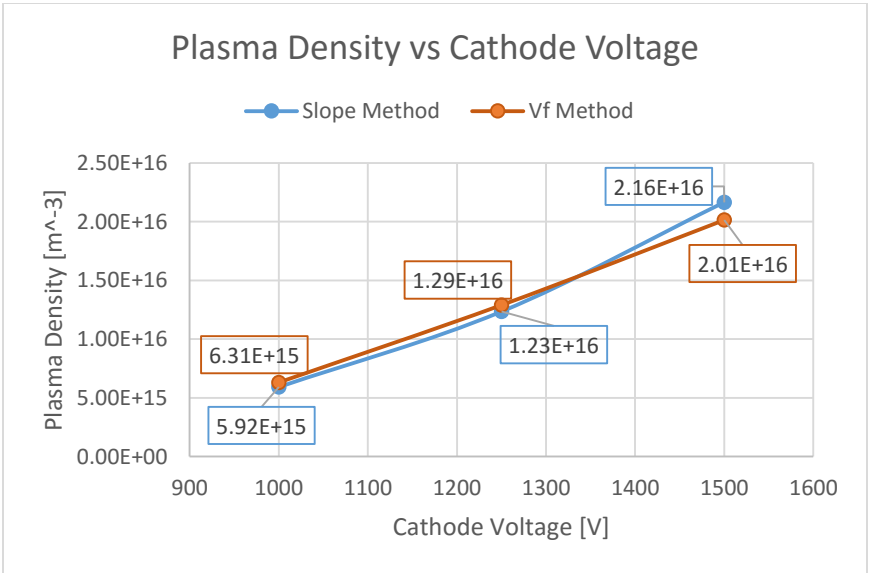

Graph 8. Plasma density of 4th version at 0.4'' away from cathode

Graph 8 of plasma density has a clear increasing tendency as cathode voltage increases. This result further confirms the expectation. By comparing two methods, even though there are some variations, the numbers are in the same magnitude and have same increasing trend. Therefore, our methods are proved to be valid. The variation is from drawing approximated slope to get Tev. On the other hand, the floating voltage is more accurate to obtain. Hence, the corresponding Tev calculated from V_F is more accurate than from slope.

3.3.3. IV Curve as Cathode Voltage Varies at 0.6''

Furthermore, plasma properties have been studied outside the confinement grid at 0.6'' away from cathode. The corresponding IV curve is shown in Graph 9 for three cathode voltages. Again, same increasing trend was found as cathode voltage increases.

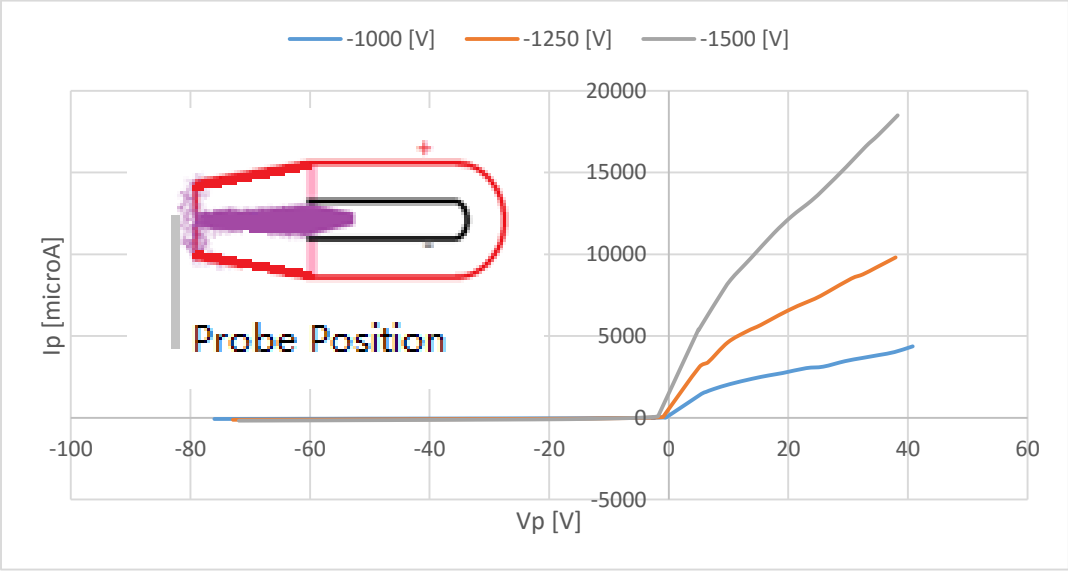

Graph 9. IV Curve for 4th version at 0.6'' away from cathode

By taking closer look at negative probe voltage region, same trend of decreasing ion current were found and illustrated in Graph 10.

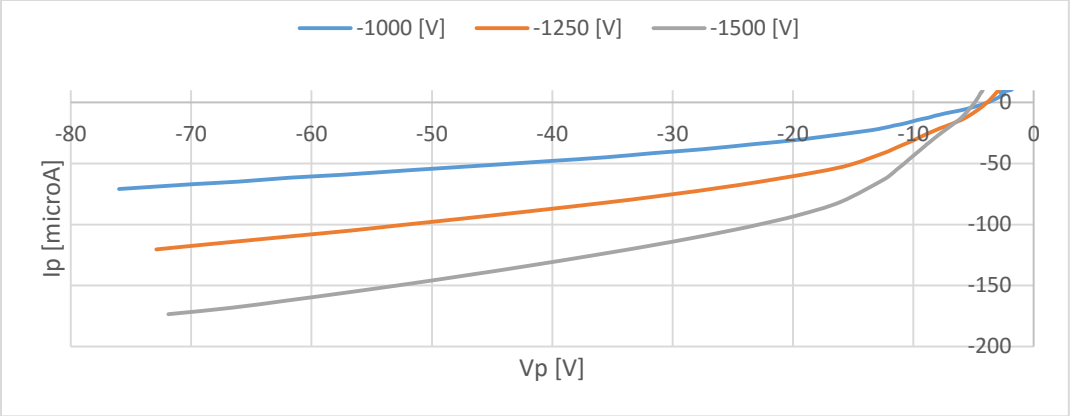

Graph 10. Ion current becomes more negative as cathode voltage increases.

Plasma properties of 4th version at 0.6'' away are shown in Table 2 for two methods. Both from Table 12 and Graph 11, the plasma density is increasing as cathode voltage increase for the same reason as discussed above. The Tev at 0.6'' is much smaller than at 0.4'' maybe because of less confinement at 0.6'' to causes less particle collision, which leads to lower electron temperature.

	Slope Method			Vf Method		
Vc [V]	1000	1250	1500	1000	1250	1500
Tev [eV]	1.73	1.77	2.25	1.90	1.90	2.33
ve,th [m/s]	8.81E+05	8.91E+05	1.00E+06	9.23E+05	9.23E+05	1.02E+06
ne [m^-3]	9.79E+15	2.44E+16	3.98E+16	9.35E+15	2.35E+16	3.91E+16

Table 2. Plasma properties summary of 4th version at 0.6'' away from cathode

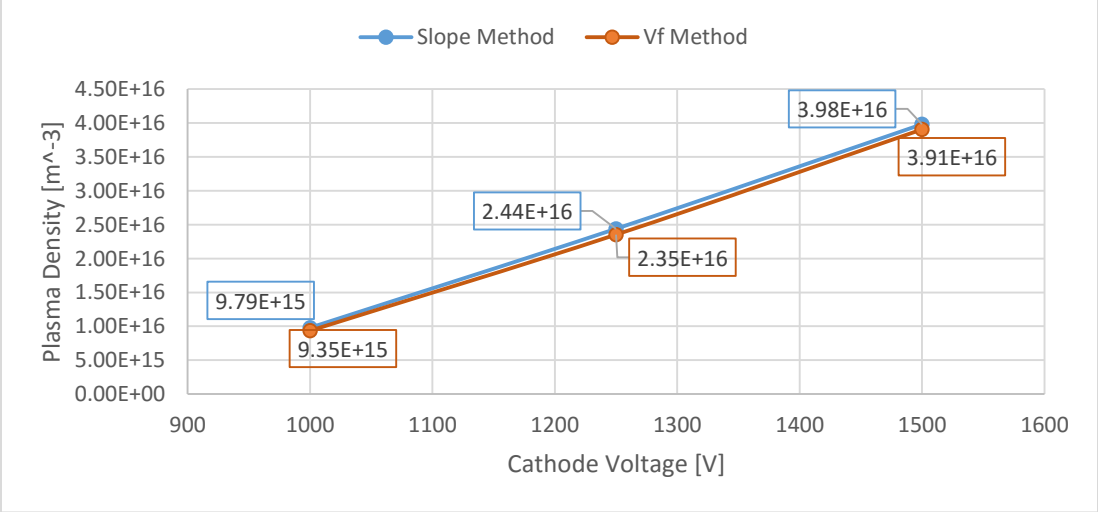

Graph 11. Plasma density of 4th version at 0.6'' away from cathode

3.3.4. IV Curve as Probe Position Varies

Total comparisons of plasma properties at 0.4'' and 0.6'' are shown in Graph 12, which indicating a decrease in Tev and ve,th, but increase in ne. Since at 0.6'' away from cathode, the plasma is injected outside of confinement grid and at week potential field, which causes less collisional electrons that have lower electron temperature. Since, the electron temperature which means their energy is decreasing as it travels outside the grid, the corresponding decreased velocity makes sense. It was expected that the plasma density would decreases once the particles leave the confinement grid. However, the data shows that the plasma density increases. This may due to the plasma tail formed at low pressure, which dominated by electrons, instead of neutral plasma cloud.

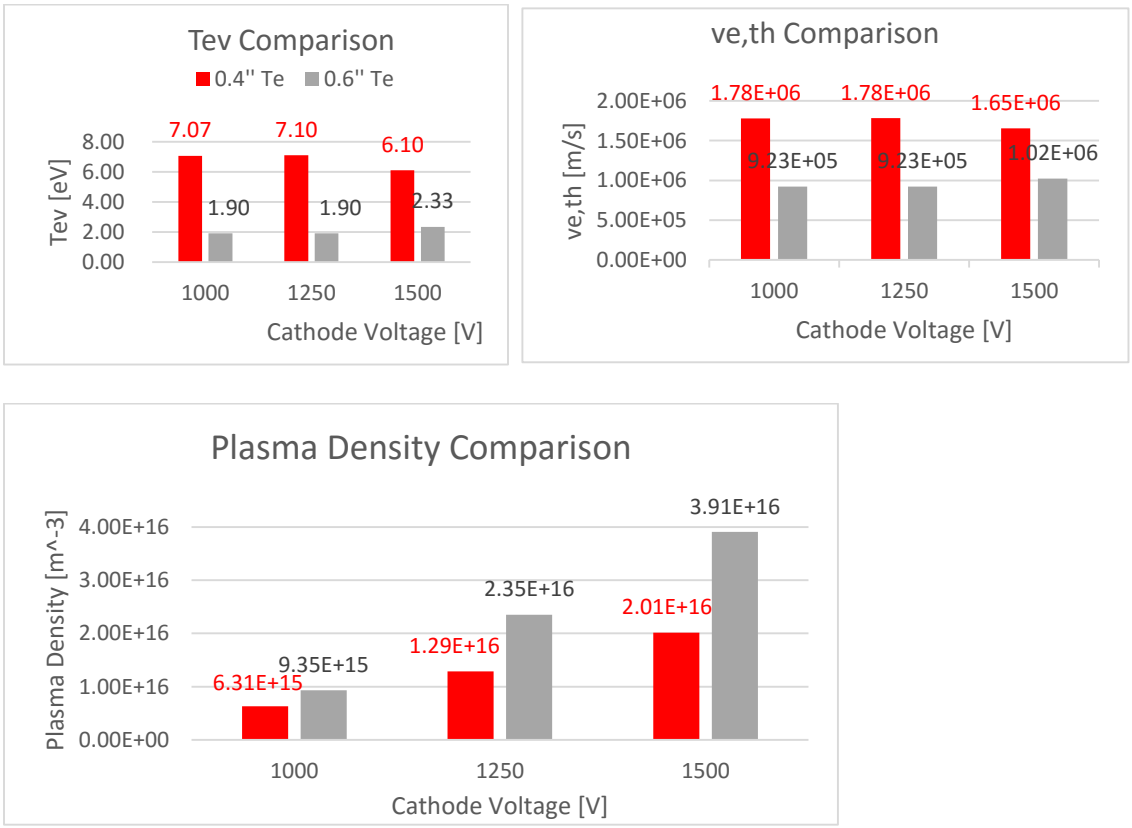

Graph 12. Total comparison of 4th version's plasma properties

4. Conclusion

In conclusion, cylindrical IEC plasma device had been studied through different versions. The plasma properties was investigated using single Langmuir probe under different discharge voltages and different positions respect to cathode grid. The final 4th version shows plasma density in the magnitude of 16 at high cathode voltage above 1 kV. By comparing to spherical IEC plasma densities measured by Tokai University and Ryan M. Meyer, 4th version plasma device has about the same plasma density. [20-21] However, in both references, the operating voltage for the grid was a lot higher than 1.5 kV. Therefore, it gives 4th version an advantage to be able to generate cold plasma using less electrical energy. The reason why it is still been called “cold plasma” is because many other high density plasma sources would able to have density in magnitude of 22 or more, for example the FRC plasm source. [22-23] However, those high density plasma sources were pulsed, not continuous. MHD operates at continuously high density plasma, which IEC plasma source would provide if its plasma density would be improved in future work. For the purpose of study plasma itself and small spacecraft thruster device, the 4th version is an excellent deign.

5. Future Work

First, for plasma density verification, it would be better to construct a double Langmuir probe to compare results with single Langmuir probe. The IV analysis procedures remain the same. It was been told by Professor Shumlak that double probe would give a more accurate result without worry about reference probe potential.

Second, the construction material of 4th version is quite consistent. Some Lanthanum and standard steel wires which causes small resistance throughout grids. Also, wires are point weld on each other, which may also enlarge resistance. Hence, it would be the best to reconstruct 4th version with continuous Tungsten wires.

6. Acknowledgement:

I would like to thank Professor Ohuchi for his forever support since my Junior year as an undergraduates. It was his enthusiast towards science and strong technical support that motivate to me to start and finish this project. As an international student living alone in USA, I see Professor Ohuchi not only as my scientific research mentors and guidance, but also as a farther figure who I admire, respect and want to become. Besides all the scientific knowledges that I had learned from him, he have told me many important life lessons and methods that would guide me to success. Therefore, I want to deeply thank Profess Ohuchi again for everything that he has done for me.

In addition, I want to thank Professor Yang who would always give me a hand when I am in need, and willing to spend the time to participate in my thesis defense. Professor Yang is also one of the best professors that I have met on campus. I really appreciated his kindness and academic supports.

Lastly, I want to point out Professor Marjorie, Professor Shumlak, Phd student YiHsun Yang, and Phd student Bo for their helps and tips towards my research. I also want to thank my parents for their financial and personal supports towards my academic studies. Even though they do not understand my research field, without my parent's trust and support, I would not achieve who I am today.

Reference:

[1] Dunbar, Brian. "Propulsion Systems of the Future." *NASA*. NASA, 14 June 2003. Web. 22 Nov. 2015.

[2] Dunbar, Brian. "Pulsed Plasma Thrusters." *NASA*. NASA, 21 May 2008. Web. 22 Nov. 2015.

[3] Dunbar, Brian. "Magnetoplasmadynamic Thrusters." *NASA*. NASA, 7 Jan. 2010. Web. 22 Nov. 2015.

[4] "The Tokamak Fusion Reactor For Magnetically Confined Nuclear Fusion." *IAltEnergy*. IAltEnergy. Web. 22 Nov. 2015. <http://www.ialtenergy.com/tokamak-fusion-reactor.html>.

[5] National Research Council, Panel on Opportunities. *Plasma Science: From Fundamental Research to Technological Applications*. Washington, DC, USA: National Academies, 1995. Web.

[6] Rack, Philip D. "Plasma Physics." (n.d.): n. pag. *Plasma Physics*. Rochester Institute of Technology. Web. 22 Nov. 2015. <http://web.utk.edu/~prack/Thin%20films/plasma.pdf>.

[7] D. W. Knight. "Gas Discharge Tubes - Introduction." *Gas Discharge Tubes - Introduction*. G3YNH, 2013. Web. 23 Nov. 2015. <http://www.g3ynh.info/disch_tube/intro.html>.

[8] Jackson, William D. "Magnetohydrodynamic Power Generator | Physics." *Encyclopedia Britannica Online*. Encyclopedia Britannica, n.d. Web. 24 Nov. 2015. <http://www.britannica.com/technology/magnetohydrodynamic-power-generator>.

[9] Arber, Tony. "Magnetohydrodynamics (MHD)." *Van Nostrand's Scientific Encyclopedia* (2005): n. pag. *Fundamentals of Magnetohydrodynamics (MHD)*. University of Warwick, Sept. 2013. Web. 23 Nov. 2015. <https://www.ucl.ac.uk/mssl/solar/summerschool13/lectures/MSSL-Arber.pdf>.

[10] "Inertial-Electrostatic Confinement of Ionized Fusion Gases." *Journal of Applied Physics* 38 (1967): 4522. Web.

[11] Abu-Hashem, Alaa. "Investigations of Ion Confinement by Direct Current Coaxial Glow Discharge." *Journal of Modern Physics* 03.01 (2012): 48-56. Web.

[12] Santarius, John F. "Inertial Electrostatic Confinement Project - University of Wisconsin - Madison." *Inertial Electrostatic Confinement Project - University of Wisconsin - Madison*. Web. 13 Nov. 2015. http://iec.neep.wisc.edu/overview.php

[13] Kulcinski, G.L., J. Weidner, B. Cipiti, R.P. Ashley, J.F. Santarius, S.K. Murali, G. Piefer, and R. Radel. "Alternate Applications of Fusion - Production of Radioisotopes." *Fusion Science and Technology* 44.2 (2003): Fusion Science and Technology, 2003, Vol.44(2). Web.

[14] Yousefi, M., V. Damideh, and H. Ghomi. "Low-Energy Electron Beam Extraction From Spherical Discharge." *Plasma Science, IEEE Transactions on* 39.11 (2011): 2554-555. Web.

[15] Gabor, D., E. A. Ash, and D. Dracott. "Langmuir's Paradox." *Nature* 176.4489 (1955): 916-19. Web. 24 Nov. 2015. <http://www.physics.csbsju.edu/370/langmuir_probe.pdf>.
[16] Conde, Luis. "An Introduction to Langmuir Probe Diagnostics of Plasmas." *An Introduction to Langmuir Probe Diagnostics of Plasmas* (n.d.): n. pag. *An Introduction to Langmuir Probe Diagnostics of Plasmas*. 28 May 2011. Web. 24 Nov. 2015. <http://plasmalab.aero.upm.es/~lcl/PlasmaProbes/Probes-2010-2.pdf>.
[17] Chen, Francis F. "Langmuir Probe." *Van Nostrand's Scientific Encyclopedia* (2005): n. pag. *Langmuir Probe Diagnostics*. University of Califo Rnia, Los Angeles, 5 June 2003. Web. 24 Nov. 2015. <http://www.seas.ucla.edu/~ffchen/Publs/Chen210R.pdf>.
[18] Robert L. Merlino. "Understanding Langmuir Probe Current-voltage Characteristics." *American Journal of Physics* 75 (2007): 1078. Web.
[19] Hansen, Stephen P. "Plasma Experiments with Commercial Gas Tubes and Some Ideas for Microwave Oven Conversions." *The Bell Jar*. The Bell Jar, 2008. Web. 24 Nov. 2015. <http://www.belljar.net/plasma.htm>.
[20] Utsumi, Michiaki, and Takuma Nishigak. "Overview of Recent IEC Studies at Tokai University." *Overview of Recent IEC Studies at Tokai University* (n.d.): n. pag. *Overview of Recent IEC Studies at Tokai University*. Tokai University, 8 July 2011. Web. 21 Nov. 2015. http://www.physics.usyd.edu.au/~khachan/IEC2011/Presentations/Utsumi.pdf
[21] Meyer, R.M., M.A. Prelas, and S.K. Loyalka. "Experimental Observations of a Spherical Transparent Cathode Glow Discharge." *Plasma Science, IEEE Transactions on* 36.4 (2008): 1881-889. Web.
[22] Tichý, Hubika, ícha, Ada, Olejníek, Churpita, Jastrabík, Virostko, Adámek, Kudrna, Leshkov, Chichina, and Kment. "Langmuir Probe Diagnostics of a Plasma Jet System." *Plasma Sources Science and Technology* 18.1 (2009): 11. Web.
[23] L. Prevosto, H. Kelly, and B. R. Mancinelli. "Langmuir Probe Diagnostics of an Atmospheric Pressure, Vortex–stabilized Nitrogen Plasma Jet." *Journal of Applied Physics* 112 (2012): 063302. Web.